Inclusive production of Λ^0 hyperons by 300-GeV protons: A dependence*

K. Heller, P. Skubic,† and O. E. Overseth
Department of Physics, University of Michigan, Ann Arbor, Michigan 48109

L. Pondrom, G. Bunce, R. Handler, R. H. March, P. Martin, and M. Sheaff
Department of Physics, University of Wisconsin, Madison, Wisconsin 53706

T. Devlin, B. Edelman, R. T. Edwards, L. Schachinger, and P. Yamin‡
Department of Physics, Rutgers, The State University, New Brunswick, New Jersey 08903*
(Received 1 July 1977)

Inclusive production of Λ^0 hyperons by 300-GeV protons has been measured at fixed production angles in the laboratory between 0 and 9 mrad and laboratory momenta from 65 to 300 GeV/c. Three different solid targets were used: beryllium, copper, and lead. The A dependence of the data is suggestive of a collision model in which the hadron loses energy and gains transverse momentum as it leaves the nucleus. The experimental results are compared to such a model, and the implications are discussed.

I. INTRODUCTION

The dependence of various high-energy processes on the atomic weight of the target nucleus (A dependence) has attracted considerable attention both experimentally and theoretically in recent years. The total absorption cross section σ_a (hadron + nucleus) behaves very nearly as $A^{2/3}$, as would be expected from an opaque disk of radius $A^{1/3}$. Measurements[1] at 60 GeV of $\sigma_a(p+A)$ give a power law $\sigma_a \propto A^{0.69}$, where the small difference between 0.69 and 0.67 can be understood in a Glauber[2] picture as slightly imperfect screening of one nucleon by another within the nucleus. More detailed studies of high-energy A-dependent phenomena have also been made. For example, inclusive particle cross sections have been measured near $p_{\parallel} = 0$ in the center-of-mass frame and at high transverse momenta as a function of A in the region up to 400 GeV (see Ref. 3) and also at an incident energy of 28.5 GeV.[4] The multiplicity of produced particles (predominantly pions) has been measured by counter techniques at various energies up to 200 GeV.[5] High-energy multiplicity studies have also been made in nuclear emulsions.[6]

The A dependence found in the high-transverse-momentum inclusive measurements was expressed by the authors[3] as a power law, in analogy with the absorption cross section: $Ed\sigma(p_\perp, A)/d^3p = I(p_\perp) A^{\alpha(p_\perp)}$, where the power $\alpha(p_\perp)$ was allowed to vary with the transverse momentum. The resulting curves at 400 GeV showed that $\alpha(p_\perp)$ increased monotonically with increasing $p_\perp$ from a value near 0.9 at $p_\perp \sim 1$ GeV/c to values exceeding unity for all secondary particles measured, and approaching 1.3 for protons at $p_\perp \sim 6$ GeV/c.[3] The trend $\alpha \to 1$ at high $p_\perp$ can be understood by supposing that these rare collisions take place between pointlike particles, where screening of one particle by another becomes negligible.[7] For α to become greater than unity in this picture a rescattering of the outgoing state is necessary. This possibility has been considered by a number of authors.[4,7,8]

The ratio of multiplicities $\langle n_A \rangle / \langle n_H \rangle$ for a nucleus A compared to hydrogen shows essentially no A dependence for forward angles in the laboratory less than 3.5°.[5] This result might appear surprising, because in a heavy nucleus such as lead the nuclear thickness is of the order of three mean-free paths, and if ten pions are produced at each interaction, 1000 pions might come out. There are good reasons from basic quantum mechanics[9] to believe that in a volume with radius of the order of the nuclear force range the highly excited hadronic state produced in the first collision does not contain a fixed number of particles. This idea has been refined by Gottfried to explain the constancy of the multiplicity.[10] In this picture the projectile, a proton for example, retains much of its protonlike character in excited form after the primary collision in the nucleus. Subsequent interactions within the nucleus are much like the primary one, hardly altering the final-state multiplicity into which the "proton" decays after leaving the nuclear volume. The multiplicity at larger angles would be expected to increase with A as a result of the excitation of target nucleons within the nucleus by the projectile. Such an increase in multiplicity at large angles is consistent with experiment.

In this paper results are reported for the A dependence of the inclusive production of Λ^0 hyperons by 300-GeV protons at Fermilab: $p + A \to \Lambda^0 + X$, where nuclear targets Be ($A = 9$), Cu ($A = 64$), and Pb ($A = 208$) were used. The inclusive Λ^0 spectra

have many leading particle characteristics, similar to those of the proton. The region of phase space studied was predominantly projectile fragmentation with $p_{lab} > 65$ GeV/c and $p_\perp \leq 1.5$ GeV/c, and hence in the same kinematic range as the multiplicity work of Ref. 5. It will be shown that the observed A dependence of Λ^0 production can be described by a simple collision model in which the outgoing excited baryon loses energy and acquires transverse momentum through collisions with other nucleons in the target nucleus.

II. APPARATUS

A plan view of the apparatus is shown in Fig. 1. Various aspects of the equipment have been described in previous reports.[11] A beam of protons at 300 GeV and typical intensity 10^7/pulse struck a solid target upstream of a sweeping magnet which cleared charged particles from the neutral beam. The neutral beam was defined by a collimating system embedded in the sweeping magnetic field. The solid angle defined was 1.2 μsr. The length of the magnetic field was 5.4 m, over which no neutral particle decays could be observed. The decay volume was a 12-m vacuum drift space, defined upstream by a veto scintillation counter and downstream by the first proportional chamber. Hyperons which decayed by the charged mode $\Lambda^0 \to p\pi^-$ in this volume were detected by the proportional chamber spectrometer, which was of standard design. Fast signals from the chambers themselves served as the trigger. An argon-filled ionization chamber was the primary monitor of the incident-proton beam flux. The nuclear targets were nominally $\frac{1}{2}$ interaction length thick. Absorption corrections for finite target thickness were obtained by studying the yield from $\frac{1}{4}$ interaction length targets. The spectrum shapes observed did not depend on target thickness.[12] Data were taken at fixed production angles in the laboratory between 0 and 8.9 mrad. The incident proton beam direction was changed in a vertical plane to vary the angle between the proton beam line and the fixed axis of the collimator.

III. RESULTS

Table I gives the invariant cross sections obtained at three production angles for the three nuclear targets, and Fig. 2 shows these cross sections divided by the $(p+A)$ absorption cross sections reported in Ref. 1, i.e., $\sigma(p\text{Be}) = 216$ mb, $\sigma(p\text{Cu}) = 812$ mb, and $\sigma(p\text{Pb}) = 1930$ mb. Events below 65 GeV/c in the laboratory have been omitted because the corrections for losses in the collimator become too large to be reliable at the lower energies.

The data were fitted to empirical functions of $x = p_\parallel^*/p_{max}^*$ and $p_\perp = p\sin\theta$ for the produced hyperon in order to interpolate between the fixed angles and obtain invariant cross sections of the form $Ed^3\sigma(x, p_\perp)/dp^3$. Satisfactory χ^2 was obtained for each fit, and the functions for each target gave accurate and convenient expressions for the measured cross sections over the kinematic range covered by the data.[13] These invariant cross sections were then used to determine the power of A from the equation

$$\frac{Ed^3\sigma}{dp^3}(A, x, p_\perp) = A^{\alpha(x,p_\perp)}\ \frac{Ed^3\sigma}{dp^3}(1, x, p_\perp). \quad (1)$$

The most complete sets of data were taken for Be ($A = 9$) and Pb ($A = 208$), and these two cross sec-

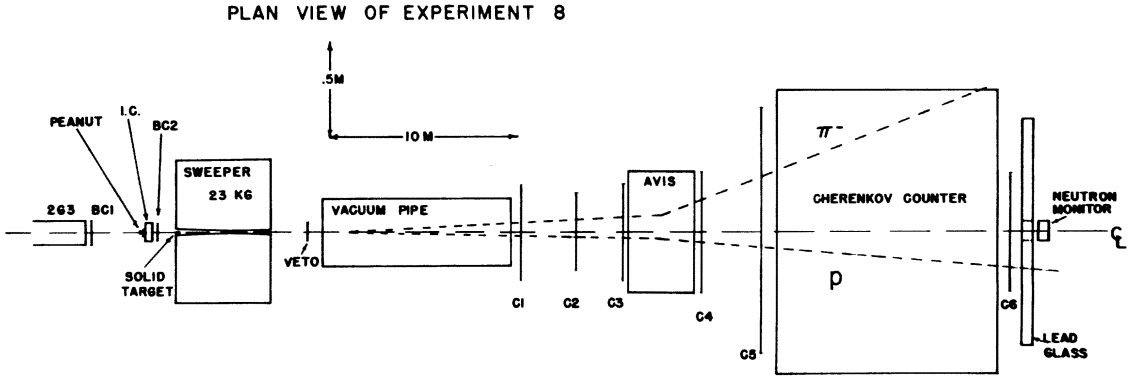

FIG. 1. Plan view of the apparatus. The first magnet shown, labeled 2G3, bends the incident proton beam in a vertical plane down onto the target to obtain various production angles. $BC1$ and $BC2$ are proportional chambers used to determine beam position. The "peanuts" were small scintillators used to count the proton flux at low intensity, and calibrate the ion chamber. I. C. Avis was a ferric superconducting magnet with aperture 20 cm × 60 cm × 2m long and $\int Bdl = 24$ kg m. The Cherenkov counter and lead-glass array were not used in this experiment.

TABLE I. Λ^0 invariant cross sections. The error given is the statistical standard deviation.

p (GeV/c)	Beryllium $Ed^3\sigma/dp^3$ (mb/GeV^2)	Copper $Ed^3\sigma/dp^3$ (mb/GeV^2)	Lead $Ed^3\sigma/dp^3$ (mb/GeV^2)
	0 mrad production angle		
65	4.39 ± 0.21	17.3 ± 1.21	35.8 ± 2.3
75	4.40 ± 0.18	16.8 ± 0.97	32.1 ± 1.7
85	4.22 ± 0.16	4.17 ± 0.76	29.5 ± 1.4
95	4.39 ± 0.16	15.4 ± 0.73	28.9 ± 1.3
105	4.31 ± 0.10	14.7 ± 0.51	24.8 ± 0.84
115	4.16 ± 0.09	13.2 ± 0.45	24.0 ± 0.77
125	4.16 ± 0.09	13.4 ± 0.43	22.2 ± 0.70
135	4.09 ± 0.09	12.2 ± 0.39	22.0 ± 0.67
145	3.89 ± 0.08	11.8 ± 0.37	20.5 ± 0.62
155	3.71 ± 0.08	10.3 ± 0.33	19.4 ± 0.58
165	3.60 ± 0.07	10.1 ± 0.31	16.8 ± 0.50
175	3.51 ± 0.07	9.80 ± 0.29	16.3 ± 0.48
185	3.32 ± 0.07	8.67 ± 0.27	15.5 ± 0.46
195	3.18 ± 0.06	7.78 ± 0.25	13.7 ± 0.42
205	2.88 ± 0.06	7.76 ± 0.25	12.4 ± 0.39
215	2.72 ± 0.06	7.07 ± 0.22	11.7 ± 0.38
225	2.55 ± 0.06	6.58 ± 0.22	10.5 ± 0.35
235	2.32 ± 0.05	5.98 ± 0.21	9.9 ± 0.34
245	2.02 ± 0.05	5.15 ± 0.19	8.7 ± 0.31
255	1.76 ± 0.04	4.67 ± 0.18	7.8 ± 0.29
265	1.47 ± 0.04	3.53 ± 0.15	6.4 ± 0.26
275	1.13 ± 0.03	3.00 ± 0.14	4.5 ± 0.21
285	0.77 ± 0.03	2.02 ± 0.11	3.1 ± 0.18
295	0.45 ± 0.02	1.22 ± 0.09	2.0 ± 0.14

p (GeV/c)	Beryllium $Ed^3\sigma/dp^3$ (mb/GeV^2)	Lead $Ed^3\sigma/dp^3$ (mb/GeV^2)
	5.3 mrad production angle	
65	3.22 ± 0.074	26.7 ± 0.99
75	2.91 ± 0.056	23.1 ± 0.71
85	2.41 ± 0.042	18.1 ± 0.50
95	2.09 ± 0.038	15.1 ± 0.41
105	1.73 ± 0.030	12.2 ± 0.32
115	1.45 ± 0.026	9.49 ± 0.26
125	1.16 ± 0.021	7.52 ± 0.21
135	0.941 ± 0.017	5.71 ± 0.17
145	0.740 ± 0.014	4.56 ± 0.14
155	0.571 ± 0.013	3.36 ± 0.12
165	0.415 ± 0.008	2.59 ± 0.09
175	0.315 ± 0.007	1.59 ± 0.07
185	0.217 ± 0.005	1.33 ± 0.06
195	0.157 ± 0.004	0.91 ± 0.05
205	0.110 ± 0.003	0.64 ± 0.04
215	0.069 ± 0.002	0.41 ± 0.03
225	0.050 ± 0.002	0.26 ± 0.02
235	0.028 ± 0.002	0.15 ± 0.02
245	0.016 ± 0.001	0.058 ± 0.011
255	0.0086 ± 0.0008	0.037 ± 0.009
265	0.0036 ± 0.0005	0.022 ± 0.007
275	0.0015 ± 0.0004	

TABLE I. (*Continued*)

p (GeV/c)	Beryllium $Ed^3\sigma/dp^3$ (mb/GeV^2)	Copper $Ed^3\sigma/dp^3$ (mb/GeV^2)	Lead $Ed^3\sigma/dp^3$ (mb/GeV^2)
	8.9 mrad production angle		
65	2.10 ± 0.05	9.65 ± 0.35	20.4 ± 0.64
75	1.61 ± 0.03	6.62 ± 0.22	13.8 ± 0.39
85	1.05 ± 0.02	4.44 ± 0.14	8.75 ± 0.25
95	0.72 ± 0.01	3.11 ± 0.10	5.94 ± 0.17
105	0.50 ± 0.01	1.92 ± 0.07	4.22 ± 0.13
115	0.316 ± 0.007	1.20 ± 0.05	2.63 ± 0.09
125	0.218 ± 0.005	0.759 ± 0.03	1.77 ± 0.07
135	0.124 ± 0.004	0.479 ± 0.02	1.02 ± 0.05
145	0.079 ± 0.003	0.304 ± 0.02	0.652 ± 0.03
155	0.046 ± 0.002	0.179 ± 0.01	0.431 ± 0.03
165	0.024 ± 0.001	0.096 ± 0.009	0.223 ± 0.02
175	0.014 ± 0.001	0.048 ± 0.006	0.116 ± 0.01
185	0.0051 ± 0.0006	0.014 ± 0.004	0.045 ± 0.008
195	0.0023 ± 0.0005	0.013 ± 0.003	0.011 ± 0.0064
205	0.0006 ± 0.0004	···	0.0009 ± 0.0064

tions were used at each $(x, p_\perp)$ to determine the exponent $\alpha(x, p_\perp)$. The Cu ($A = 64$) data then furnished a check on the validity of the power-law hypothesis. This check was always satisfactory, indicating that Eq. (1) was a good parametrization of the data. Table II gives the power $\alpha(x, p_\perp)$ so obtained as a function of $p_\perp$ for various values of x and Fig. 3 shows a plot of the results. Note that since $\sigma_a(p+A)$ varies as $A^{0.69}$, and most values of α are below this number, the observed invariant cross sections actually increase less rapidly with increasing A than the overall absorption cross section. Only at the lowest value of x ($x = 0.2$) does this trend reverse, and α exceed 0.69. The 300-GeV proton data of Ref. 3 are also shown in Fig. 3 for comparison. The trend of increasing α with decreasing x continues into $x = 0$, and it is clear that the data of Ref. 3 and the present experiment are in qualitative agreement. This same general behavior of α as a function of x has also been observed in the high-energy production of $\rho + \omega$ vector mesons.[14]

It is convenient to use the longitudinal rapidity variable y rather than x to display the invariant phase space available. The rapidity is defined by

$$y = \tfrac{1}{2} \ln \frac{E + p_\parallel}{E - p_\parallel} , \tag{2}$$

and has the convenient property that the invariant phase-space element loses its energy denominator:

$$\frac{d^3\vec{p}}{E} = \pi dy dp_\perp{}^2 . \tag{3}$$

Thus the invariant cross sections expressed in terms of $(y, p_\perp{}^2)$ can be directly integrated to give the multiplicity. The data displayed in Fig. 2 are

TABLE II. Results of the power-law hypothesis.

$$E\frac{d^3\sigma}{dp^3}(A) = A^{\alpha(x,p_\perp)} E\frac{d^3\sigma}{dp^3}(A = 1)$$

$p_\perp$ (GeV/c)	$x = 0.2$ α	$x = 0.4$ α	$x = 0.6$ α	$x = 0.8$ α
0	0.676 ± 0.014	0.553 ± 0.014	0.480 ± 0.014	0.456 ± 0.014
0.25	0.685 ± 0.014	0.563 ± 0.014	0.490 ± 0.014	0.465 ± 0.014
0.50	0.708 ± 0.014	0.584 ± 0.014	0.506 ± 0.014	0.471 ± 0.014
0.75	0.748 ± 0.014	0.619 ± 0.014	0.532 ± 0.014	0.479 ± 0.014
1.00	···	0.673 ± 0.014	0.571 ± 0.014	0.492 ± 0.016
1.25	···	···	0.625 ± 0.015	0.511 ± 0.020
1.50	···	···	0.685 ± 0.020	0.528 ± 0.028
1.75	···	···	···	0.520 ± 0.070

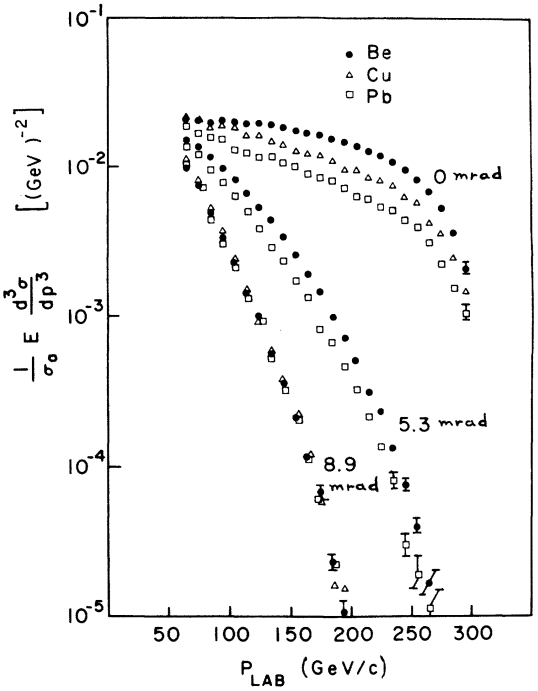

FIG. 2. Inclusive cross sections for $p+A \rightarrow \Lambda^0+X$ at constant angle divided by the absorption cross sections of Denisov *et al.* (Ref. 1). The statistical errors are of the order of the size of the points except at very high value of p_{lab}, where typical errors are shown. There is an absolute uncertainty in normalization of ± 6% which is not shown.

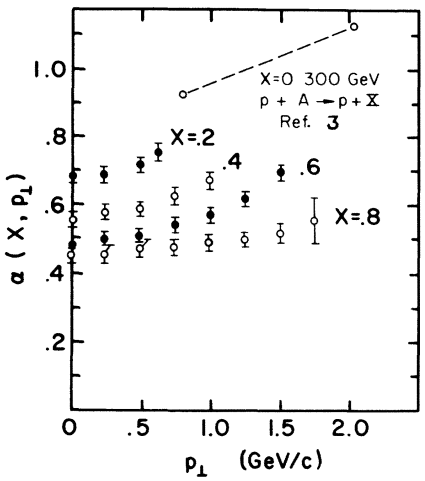

FIG. 3. Results using the interpolated beryllium and lead data to obtain the power-law A dependence of Eq. (1). Note that over most of the kinematic range studied $\alpha(x,p_\perp) < 0.69$, indicating that the differential multiplicity decreases with increasing A. Because the data were taken at fixed angles, the end points in x and $p_\perp$ are correlated. Also shown are two of the low-$p_\perp$ data points from Ref. 3.

invariant cross sections divided by the absorption cross section, and hence the differential multiplicities. In terms of rapidity, these cross sections are

$$\frac{1}{\pi}\frac{d^2n}{dy\,dp_\perp^2} = \frac{1}{\sigma_a} E \frac{d^3\sigma}{d\vec{p}^3} . \tag{4}$$

Integration of this expression over all phase space gives the average multiplicity, the average number of particles—in this case Λ^0's—produced per interaction. Thus

$$\langle n \rangle = \int_{y_{min}}^{y_{max}} dy \int_0^{p_{\perp max}^2} dp_\perp^2 \frac{d^2\sigma}{dy\,dp_\perp^2} . \tag{5}$$

Longitudinal rapidities are additive for Lorentz transformations along the incident-particle axis, so the shape and total width of the curve in rapidity is Lorentz invariant. For definiteness, assume that the nucleon-nucleon center-of-mass frame is appropriate. Figure 4 then shows the 0-mrad points in Fig. 2 replotted as a function of center-of-mass rapidity y_c. Also shown is the extrapolated "nucleon" cross section obtained from the beryllium and lead cross sections via Eq. (1). For normalization this cross section has been divided by the extrapolated $\sigma_a(pp) = 46$ mb obtained from the complex nuclear cross sections of Ref. 1 rather than the true value $\sigma_a(pp) = 33$ mb. Note that about half of the available forward-hemisphere phase space is missing because of the 65-GeV/c cut on laboratory momentum. This emphasizes the fact that this experiment is predominantly a study of projectile fragmentation.

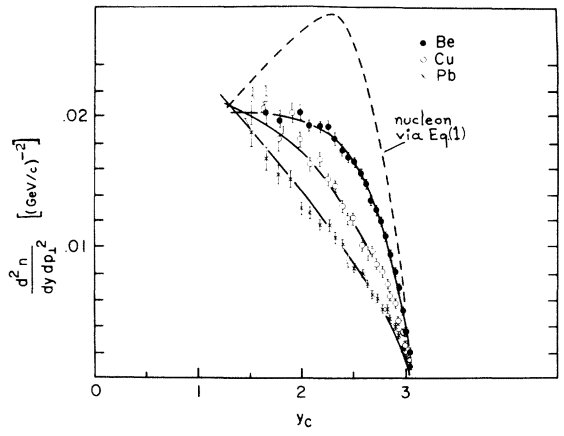

FIG. 4. Double-differential multiplicity as a function of nucleon-nucleon center-of-mass rapidity at $p_\perp = 0$ for the three nuclear targets. The functional fits mentioned in the text to these data points are shown as solid lines. Also shown is the extrapolated "nucleon" distribution obtained from the beryllium and lead cross sections via Eq. (1).

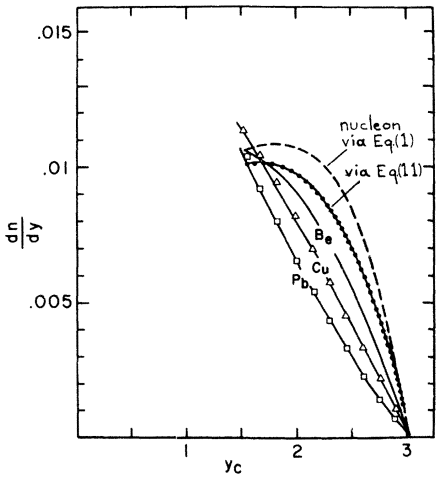

FIG. 5. The solid curves give the results of integration of the differential multiplicities over $p_\perp^2$. The triangles and the squares are the predictions for the copper and lead distributions, respectively, using the collision model discussed in the text and the beryllium curve. The dashed curve is the extrapolated nucleon spectrum based on Eq. (1), and the curve with dots is the same spectrum from Eq. (11).

Figure 4 clearly shows that the differential multiplicity decreases with increasing A for $y_c > 1.5$, that the curves cross around $y_c = 1.5$, which is the middle of the forward hemisphere, and that a natural extrapolation into small y would be a differential multiplicity which increases with increasing A. In this manner the total multiplicity $\langle n \rangle$ could be A independent, consistent with the pion data of Ref. 5. The average energy loss between Be and Pb displayed in the figure is about 6% i.e., 18 GeV. This fraction must appear at large angles in pions from the target nucleons, where the multiplicity is known to increase rapidly with increasing A.[5] It is interesting to note that lower-energy data for proton spectra produced by 24-GeV protons on the same target nuclei show the same general A dependence, and the same fractional energy transfer to the nucleus between Be and Pb.[15] Figure 5 shows the result of integrating the functional forms for the three invariant cross sections over the $p_\perp^2$ variable. The A dependence of the single differential multiplicity dn/dy resembles that of the double differential at $p_\perp^2 = 0$

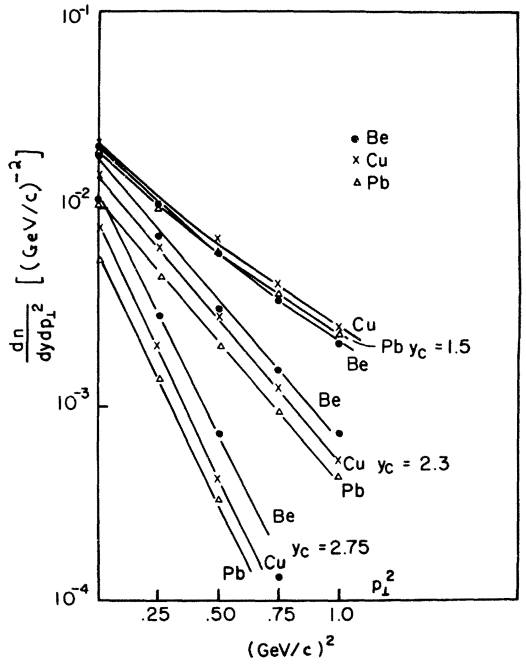

FIG. 6. Double-differential multiplicities plotted as a function of $p_\perp^2$ for various fixed values of y. The interpolated fits to the data were used to generate the points shown for the three targets. The lines are to guide the eye. Only at low y is an A dependence as a function of $p_\perp^2$ apparent.

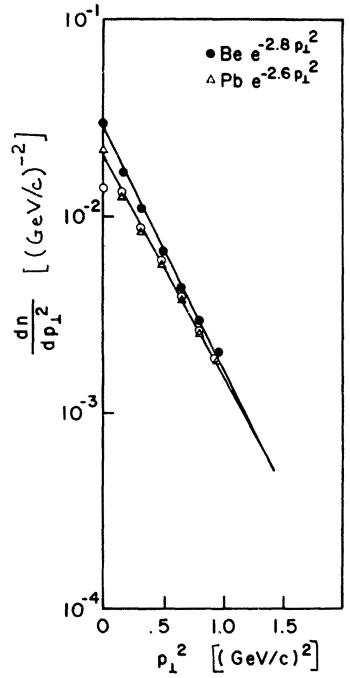

FIG. 7. Differential multiplicity $dn/dp_\perp^2$ vs $p_\perp^2$. Beryllium and lead are shown, with slopes $-2.8/(\text{GeV}/c)^2$ and $-2.6/(\text{GeV}/c)^2$, respectively, indicating a slight tendency for the distribution in transverse momentum to become shallower as A increases. The open circles are the result of the calculation of the lead spectrum from beryllium using the collision model discussed in the text.

because the A dependence is not a strong function of transverse momentum, and the yield drops exponentially with increasing $p_\perp{}^2$.

These features are shown by the companion curves as a function of $p_\perp{}^2$, Fig. 6 and 7. Figure 6 gives the double differential $d^2n/dydp_\perp{}^2$ for three different values of y vs $p_\perp{}^2$, and Fig. 7 gives the results of integration over the rapidity range $1.5 \leq y \leq 3.0$. At fixed y the curves in Fig. 6 are approximately exponential in $p_\perp{}^2$, with a slope which increases as y increases. There is a tendency (very slight at large y, stronger near $y = 1.5$) for the lead data to approach the beryllium data as $p_\perp{}^2$ increases; that is, the slope of the lead data is somewhat shallower. The integrated curves $dn/dp_\perp{}^2$ are characterized by a single exponential in $p_\perp{}^2$ for $0 \leq p_\perp{}^2 \leq 1$ GeV^2.

These features of the A dependence exhibited by Figs. 4, 5, 6, and 7 are strongly suggestive of a collision process, where the excited baryonic state which eventually decays into the observed Λ^0 loses in rapidity and gains slightly in $p_\perp{}^2$ by interaction with target nucleons on its way out of the nucleus.

IV. ANALYSIS

In the spirit of the energy-flux-cascade model of Gottfried (Ref. 10) it is natural to take the inclusive proton distributions $p+p \to p+X$ as a guide for the rapidity and transverse-momentum dependence of the collisions, since the final-state hadronic matter is protonlike. This has the added advantage that the order in which collisions take place within the nucleus is irrelevant. The number of collisions can be estimated from the average number of absorption mean free paths encountered by the incident particle in going through the nucleus as defined by Ref. 5:

$$\bar{\nu} = A\sigma_{hN}/\sigma_{hA} . \tag{6}$$

Here A is the atomic weight of the nucleus in question, and σ_{hN}, σ_{hA} are the absorption cross sections for the incident hadron on a nucleon and on nucleus A, respectively. The significance of this formula can be grasped by considering two extreme cases. The numerator is the total area which A nucleons present to the incident hadron if they do not screen each other. Thus if the nucleons were nonoverlapping disks in a plane normal to the incident hadron, then the denominator would equal the numerator, and $\bar{\nu} = 1$. If on the other hand the nucleons were distributed in a line along the beam axis, screening each other perfectly, then $\sigma_{hA} = \sigma_{hN}$, and $\bar{\nu} = A$. In this formula it is appropriate to use the true cross section in hydrogen, $\sigma_{pN} = 33$ mb. This number together with the absorption cross sections of Ref. 1, namely $\sigma_{p\,\mathrm{Be}} = 216$ mb, $\sigma_{p\mathrm{Cu}} = 812$ mb, and $\sigma_{p\mathrm{Pb}} = 1930$ mb leads to the values $\bar{\nu}_{\mathrm{Be}} = 1.4$, $\bar{\nu}_{\mathrm{Cu}} = 2.6$, and $\bar{\nu}_{\mathrm{Pb}} = 3.6$. Taking Be as the "fundamental" nucleus, there is approximately one extra collision in copper and two extra collisions in lead.

Suppose then that a baryon in a single collision acquires a distribution $f(y, p_\perp{}^2)$ in rapidity and transverse momentum. Since the baryon is not lost, the function is normalized to unity:

$$\int_{y_{\min}}^{y_{\max}} dy \int_0^{p_{\max}{}^2} dp_\perp{}^2 f(y, p_\perp{}^2) = 1 . \tag{7}$$

If the function can be separated into a product $f(y, p_\perp{}^2) = f_1(y) f_2(p_\perp{}^2)$, which is only approximately true for inclusive distributions, then f_1 and f_2 are each separately normalized to unity. Two folding functions $F_1(y - y')$ and $F_2(p^2 - p_\perp'{}^2)$, obvious extensions of f_1 and f_2, can be used to obtain the final distribution after one collision:

$$\frac{d^2n_1}{dydp_\perp{}^2} = \int_{y_{\min}}^{y_{\max}} dy' \int_0^{p_{\max}{}^2} dp_\perp'{}^2 F_1(y - y') \times F_2(p_\perp{}^2 - p_\perp'{}^2) \frac{d^2n_0}{dy'\, dp_\perp'{}^2} . \tag{8}$$

Here $d^2n_0/dy'\, dp_\perp'{}^2$ represents the distribution incident, and $d^2n_1/dydp_\perp{}^2$ the final distribution after collision. Because of the normalization condition and separation in to F_1F_2, it is irrelevant whether double differentials as in Eq. (8) or single differentials of the form dn/dy are used, since

$$\frac{dn_1}{dy} = \int_{y_{\min}}^{y_{\max}} dy' \, F_1(y - y') \frac{dn_0}{dy'} \tag{9}$$

follows from Eq. (8) upon integration over $p_\perp{}^2$.

The function $F_1(y - y')$ was obtained numerically from the data of Fig. 5 using the assumption beryllium + one collision = copper. The results are shown in Fig. 8. Note that $F_1(y - y')$ has a sharp "diffraction peak" and a rather flat continuum at lower rapidity, suggestive of the data obtained for the inclusive process $p+p \to p+X$.[16] The results of applying this function to the beryllium data once to obtain copper and twice to obtain lead are also shown in Fig. 5, and it is clear that the shapes of the curves are satisfactorily reproduced by this procedure.

A natural choice for the folding function $F_2(p_\perp{}^2 - p_\perp'{}^2)$ is an exponential in transverse momentum. The data of Ref. 16 suggest a function of the form

$$F_2(p_\perp{}^2 - p_\perp'{}^2) = be^{-b(p_\perp{}^2 - p_\perp'{}^2)} \tag{10}$$

where $b \approx 10/(\mathrm{GeV}/c)^2$. Such a steep slope for F_2 would have little effect on the beryllium distribution shown in Fig. 7, where the slope is $2.8/(\mathrm{GeV}/c)^2$, and indeed the beryllium and lead dis-

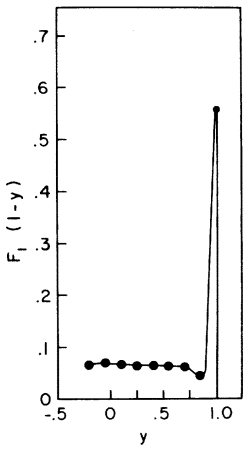

FIG. 8. Distribution in rapidity of the scattered system if the incident hadron has $y=1$. This function is qualitatively the same as $pp \to pX$ distribution of Ref. 16 for low multiplicity. The dots were obtained numerically from the data on beryllium and copper, and then used to predict lead. The line is drawn to guide the eye. The results are shown in Fig. 5.

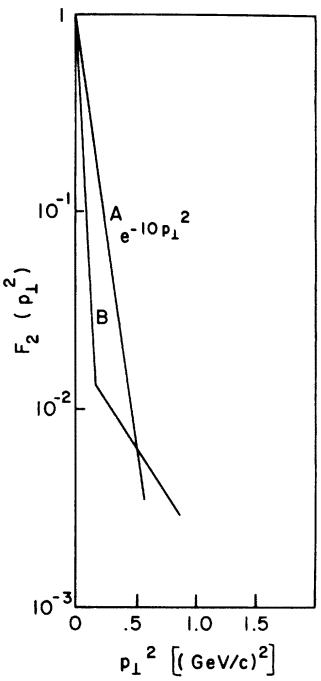

FIG. 9. Distribution in transverse momentum squared for a simple exponential $e^{-10p_\perp^2}$ and the empirically obtained "best" folding function, which has a steeper slope near $p_\perp = 0$.

tributions in $p_\perp^2$ are very similar. Straightforward application of F_2 in Eq. (10) to $dn/dp_\perp^2$ for beryllium gives the results shown as open circles in Fig. 7, and reproduces the slope of the lead data very well everywhere except at very small $p_\perp^2 \lesssim 0.1$ (GeV/c)^2. This defect is perhaps not serious in such a simple scattering model. It can be removed by obtaining an empirical F_2, as was done for F_1, from the data themselves. Such a function has a very steep slope at small $p_\perp^2$, and then a break. Equation (10) and this empirical F_2 are both shown in Fig. 9.

Equation (1) is not the most convenient way to express the A dependence in a collision model, because integrals of the form of Eq. (8) become very awkward with the A dependence in exponential form. An alternate expression proposed by several authors (Ref. 3 and 8 for example) is a polynomial in powers of $A^{1/3}$. In terms of rapidity alone the cross section may be written in the approximate form

$$\frac{d\sigma}{dy} = a(y)A^{2/3} + b(y)A + c(y)A^{4/3}. \qquad (11)$$

The first term can be interpreted as a contribution from the primary interaction, which behaves like the dominant part of the total absorption cross section—essentially as $A^{2/3}$. The second term can be thought of as having two parts: one from a primary interaction between pointlike objects, which is very rare, and a second from a rescattering of the outgoing system produced by the $A^{2/3}$ dependence. In this latter case the rescattering depends on the nuclear thickness, or $A^{1/3}$, giving an overall A^1 dependence. In this spirit the $A^{4/3}$ part can be imagined as the $A^{1/3}$ rescattering correction applied to the pointlike primary term. Thus an expansion of the form of Eq. (11) with coefficients which depend on $p_\perp$ rather than y, appropriate for the high-$p_\perp$ data of Ref. 3, must have a very large term $c(p_\perp)$ to give a dependence which approaches $A^{4/3}$. For the present experiment at low $p_\perp$ and away from the central region in y, however, this c term should be very small, since the primary interactions behave predominantly as $A^{2/3}$. Equation (11) can be cast in the form of an expansion in terms of the number of collisions by dividing by σ_a, which varies roughly as $A^{2/3}$, giving a differential multiplicity which has a term independent of the number of collisions [corresponding to a (y)], and terms linear and quadratic in the number of collisions [corresponding to $b(y)$ and $c(y)$, respectively].

Since there are three nuclei in the present experiment and three unknown functions a, b, c in Eq. (11), these functions can be found at each value of y with no constraints. The results of solving the three linear equations are shown in Fig. 10. Note that the function $c(y)$ is indeed very small, as expected. The $b(y)$ term is negative

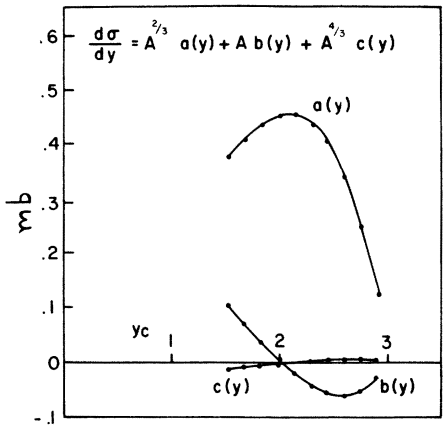

FIG. 10. Results of the inversion of Eq. (11) for the three nuclear targets to obtain coefficients $a(y)$, $b(y)$, and $c(y)$ in units of mb. According to Eq. (11), the "nucleon" distribution should be $a+b+c$, and this divided by 46 mb is plotted in Fig. 5.

because as A increases the rapidity spectrum is depressed. The extrapolated "nucleon" cross section from this expansion is obtained by setting $A=1$ in Eq. (11): $d\sigma/dy = a(y)+b(y)+c(y)$. This expression divided again by 46 mb—the extrapolated absorption cross section for p+nucleon—is shown in Fig. 5 for comparison to the extrapolation obtained through the power law Eq. (1). It is clear that although the two parametrizations Eq. (1) and Eq. (11) agree with the data, they give slightly different extrapolations to $A=1$.

V. CONCLUSIONS

Inclusive production of Λ^0 hyperons by 300-GeV protons has been studied on three different target nuclei, beryllium, copper, and lead. With regard to the propagation of an excited baryonic state through nuclear matter, copper is approximately one collision length thicker than beryllium, and lead in turn is one collision length thicker than copper. A simple collision model based on this property and using distributions characteristic of high-energy proton inclusive reactions as a guide has been applied to the data and shown to reproduce the experimental observations satisfactorily. The model is not known to the authors to be in contradiction with other experimental data on A dependence.

ACKNOWLEDGMENTS

Dr. C. Brown and Dr. H. Haggerty and the entire staff of the Meson Laboratory at Fermilab furnished the support necessary to obtain the measurements. Discussions with Dr. L. Voyvodic have been most helpful. One of the authors (L.P.) profited considerably over an extended period by discussions with Dr. B. Durand.

*Work supported in part by the National Science Foundation and the U. S. Energy Research and Development Administration.

†Present address: Rutgers, the State University, New Brunswick, New Jersey, 08903.

‡Present address: Brookhaven National Laboratory, Upton, New York, 11973.

[1]S. P. Denisov *et al.*, Nucl. Phys. B61, 62 (1973).

[2]R. J. Glauber, in *High Energy Physics and Nuclear Structure*, edited by G. Alexander (North-Holland, Amsterdam, 1967), p. 311. See also S. D. Drell and J. S. Trefil, Phys. Rev. Lett. 16, 552 (1966).

[3]L. Kluberg *et al.*, Phys. Rev. Lett. 38, 670 (1977); J. W. Cronin *et al.*, Phys. Rev. D 11, 3105 (1975).

[4]U. Becker *et al.*, Phys. Rev. Lett. 37, 1731 (1976).

[5]W. Busza *et al.*, Phys. Rev. Lett. 34, 836 (1975); W. Busza *et al.*, Paper 348 contributed to the XVIII International Conference on High Energy Physics, Tbilisi, USSR, 1976 (unpublished).

[6]J. R. Florian *et al.*, Phys. Rev. D 13, 558 (1976).

[7]G. R. Farrar, Phys. Lett. 56B, 185 (1975).

[8]J. H. Kühn, Phys. Rev. D 13, 2948 (1976).

[9]L. D. Landau, Izv. Akad. Nauk SSSR 17, 51 (1953).

[10]K. Gottfried, Phys. Rev. Lett. 32, 957 (1974).

[11]K. Heller *et al.*, in *Particles and Fields*—1975, Proceedings of the meeting of the Division of Particles and Fields of the APS, Seattle, edited by H. J. Lubatti and P. M. Mockett (Univ. of Washington, Seattle, 1976), p. 344. This reference gives the inclusive cross-section data in preliminary form. Also, G. Bunce *et al.*, Phys. Rev. Lett. 36, 1123 (1976).

[12]The correspondence between multiple collisions in a single nucleus and multiple collisions in a thick target discussed by M. L. Good *et al.*, [Phys. Rev. D 15, 1920 (1977)] if present in these data was too small to be ovserved.

[13]For more details regarding the fits to empirical functions and the reduction of the experimental data see P. Skubic, University of Michigan Report No. UM-HE-77-32, 1977 (unpublished). The function for the beryllium invariant cross section is

$$Ed^3\sigma/dp^3 = (1-x)^{0.74+0.61p_\perp{}^2} \times \exp(1.45-0.79x^2+1.28x - 1.09xp_\perp - 2.21p_\perp{}^2+0.45p_\perp{}^4),$$

and for lead is

$$Ed^3\sigma/dp^3 = (1-x)^{0.73+0.91p_\perp{}^2} \times \exp(4.11+1.1x^2-1.8x-0.92xp_\perp - 1.84p_\perp{}^2+0.56p_\perp{}^4-0.09p_\perp{}^6).$$

[14]M. Binkley *et al.*, Phys. Rev. Lett. 37, 571 (1976).

[15]T. Eichten *et al.*, Nucl. Phys. B44, 333 (1972). The relevance of this reference was kindly pointed out by L. Voyvodic.

[16]J. Whitmore *et al.*, Phys. Rev. D 11, 3124 (1975).